Supporting Information

QD-Biopolymer-TSPP Assembly as Efficient BiFRET Sensor for Ratiometirc and Visual Detection of Zinc Ion

Yuqian Liu,[a] Xiaojun Qu,[a] Qingsheng Guo,[a] Qingjiang Sun,[a*] and Xuebin Huang[b*]

[a]State Key Laboratory of Bioelectronics, School of Biological Science & Medical Engineering, Southeast University, Nanjing 210096, P. R. China
[b]School of Chemistry and Chemical Engineering, Beijing Institute of Technology, Beijing 100081, P. R. China

*Fax: (86) 25-83792349. Email: sunqj@seu.edu.cn; huangxb@bit.edu.cn

Contents:

Table S1. Comparison of analytical parameters and mechanisms of different fluorescent Zn^{2+} sensors.

Sensor	Ratiometric	LOD	Range	Mechanism	Reference
QD-poly(dA)-TSPP	Yes	1 nM	0.05-4 μM	BiFRET	This work
QD@SiO_2@TSPP	Yes	60 nM	0.3-6.0 μM	BiFRET	*Anal. Chem.* **2015**, *87*, 5318
QD/zincon	No	0.57 μM	10-1000 μM	FRET	*Analyst* **2009**, *134*, 159
CD-QCT	No	2 μM	2-100 μM	FRET	*Microchim. Acta* **2015**, *182*, 2443
Rhodamine derivative	Yes	40 nM	0.2-20 μM	FRET	*Anal. Chem.* **2010**, *82*, 3108
QD-Azamacrocycle	No	2.4 μM	5-500 μM	PHT	*Anal. Chem.* **2008**, *80*, 8260
QD-DPA-P-DTC	No	0.7 μM	0.9-16 μM	PHT	*Analyst* **2013**, *138*, 2181
QD@SiO_2@QD-Phen	Yes	1.1 μM	5-100 μM	PHT	*RSC Adv.* **2015**, *5*, 69251
SiNP–PEIQ	Yes	0.5 μM	2.0-20 μM	PET	*Biosens. Bioelectron.* **2014**, *61*, 397
AuNC-BSA	Yes	29 nM	0.1-100 μM	PET	*Biosens. Bioelectron.* **2015**, *74*, 322
2-picolylamine derivative	Yes	7.2 nM	0-5.0 μM	PET	*RSC Adv.* **2015**, *5*, 57141
6-substituted quinoline	Yes	2.5 μM	N/A	ICT	*Chem. Commun.* **2012**, *48*, 4196

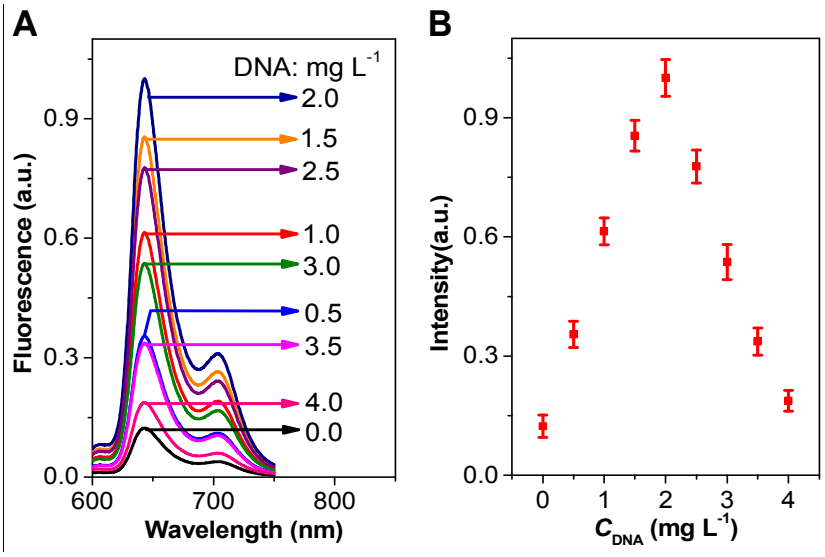

Figure S1. (A) Fluorescence spectra of TSPP for the ^{517}QD-DNA-TSPP assemblies with varying DNA coatings. (B) The emission intensity of TSPP as a function of the DNA amount.

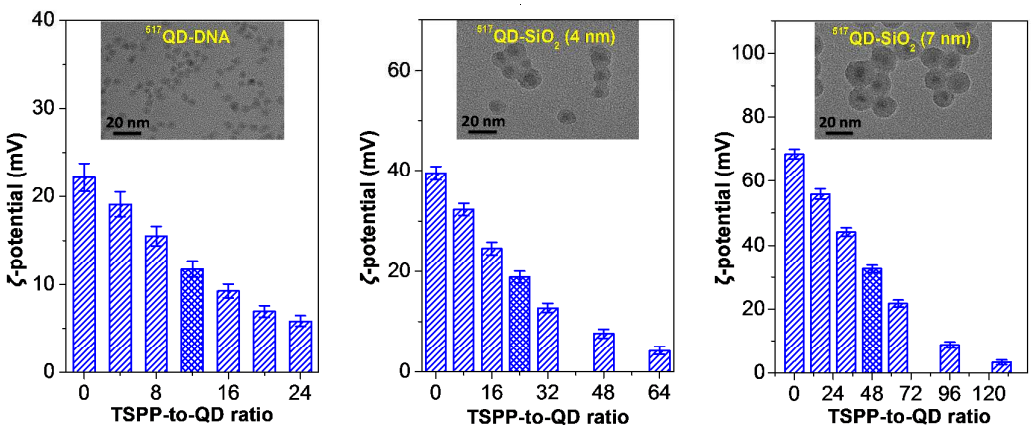

Figure S2. Evolution of ζ-potentials of ^{517}QD-DNA, ^{517}QD-SiO_2 (4 nm) and ^{517}QD-SiO_2 (7 nm) as a function of TSPP-to-QD ratio. The insets show TEM images of the QD coated with different spacers/thicknesses.

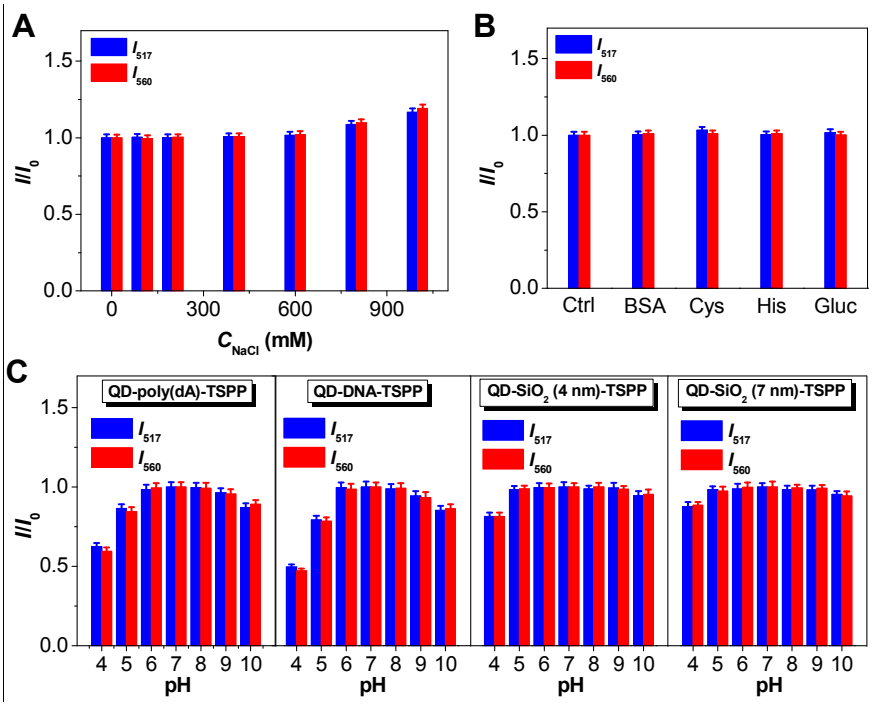

Figure S3. Stability of the QD-BiFRET sensor with respect to (A) varying NaCl concentrations, (B) various biomolecules, and (C) varying pH values.

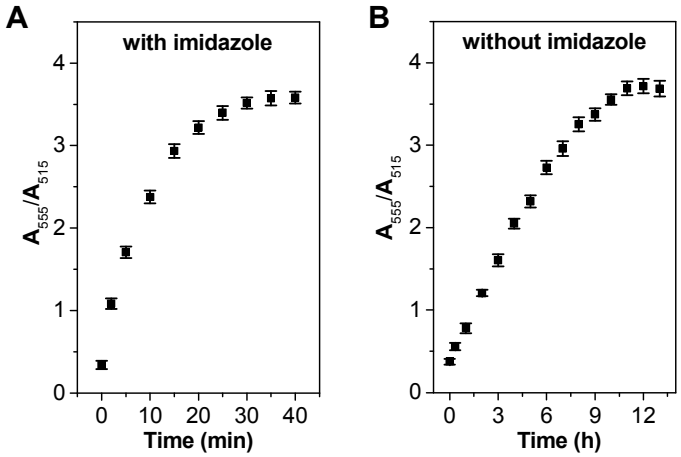

Figure S4. Changes of the ratio of 555 nm-to-515 nm absorbance with respect to time upon treating 4.0 μM TSPP with 6.0 μM Zn^{2+}: (A) with and (B) without 60 mM imidazole.

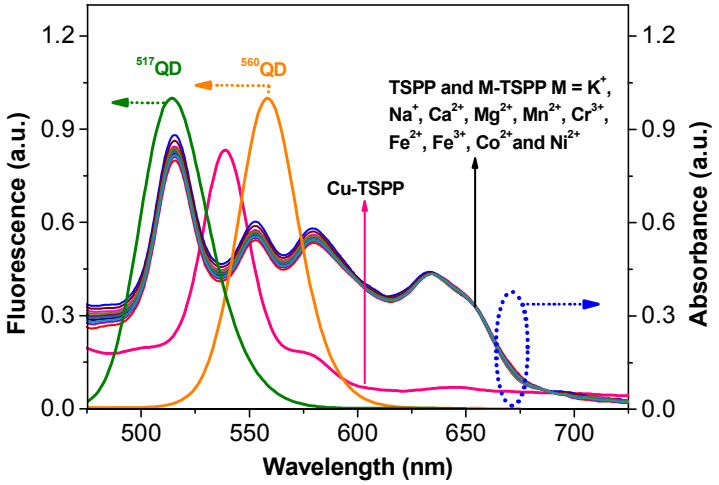

Figure S5. Fluorescence spectra of ^{517}QD and ^{560}QD, and absorption spectra of TSPP upon treating with various metal ions.

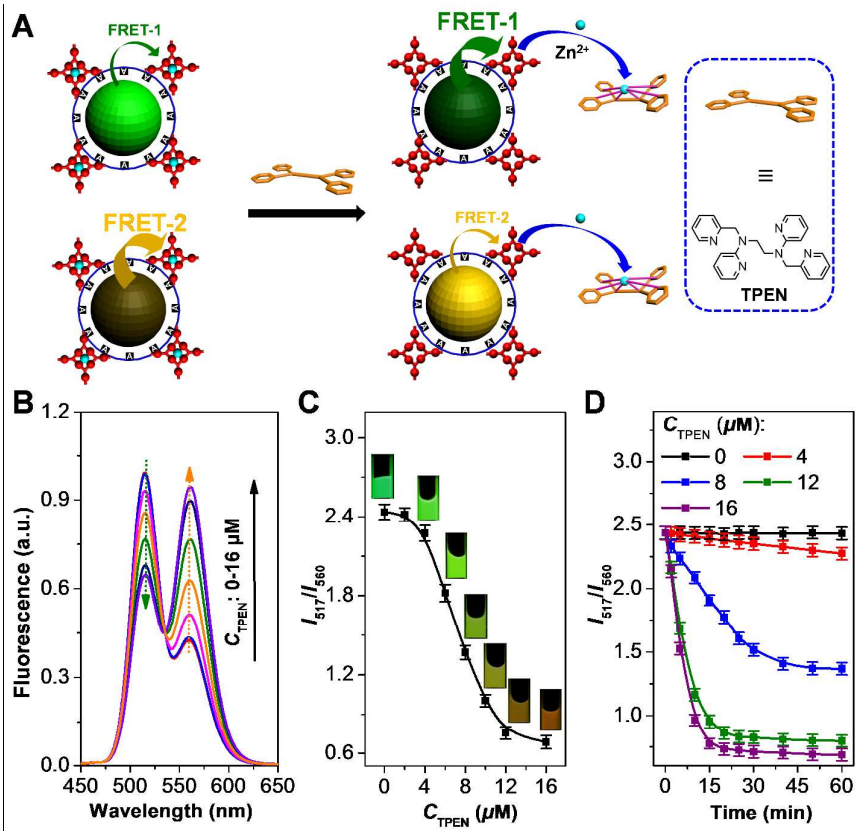

Figure S6. (A) Schematic illustration of the reversibility of QD-BiFRET sensor upon the addition of TPEN. (B) Fluorescence spectra of 6 μM Zn^{2+}-responded QD-BiFRET sensor upon the addtion of 0-16 μM of TPEN. (C) Evolution of the ^{517}QD-to-^{560}QD emission ratio and the emission color of sensor solution as a function of the TPEN concentration. (D) Evolution of relative ^{517}QD-to-^{560}QD emission ratio of 6 μM Zn^{2+}-responded QD-BiFRET sensor with respect to time upon exposure of different amounts of TPEN.

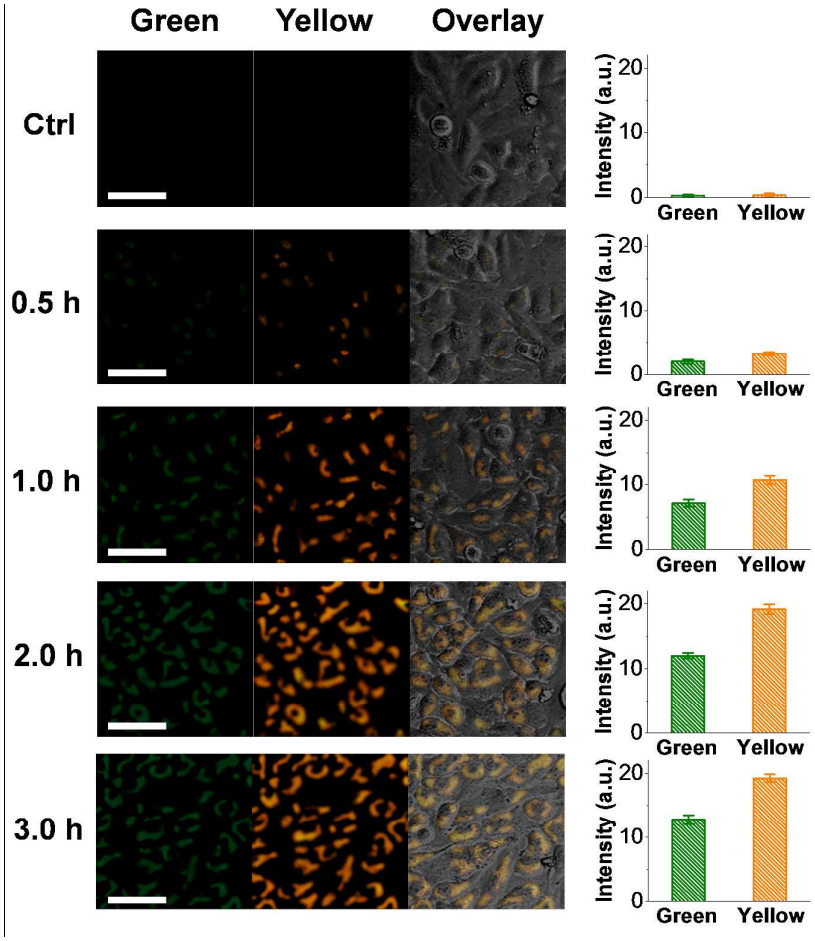

Figure S7. Fluorescent (green-channel and yellow-channel) images of live HeLa cells incubated with the QD-BiFRET sensor for different time. Scale bar: 30 μm. Histograms showing intensities of green and yellow emissions in the cells.